

Edge Vortices—Some Observations and Discussion of the Phenomenon," ARC R & M 3282, April 1961, Aeronautical Research Council, England.

¹³ Finlayson, B. A., *The Method of Weighted Residuals and Variational Principles*, Academic Press, New York, 1972.

¹⁴ Morton, B. R., "Geophysical Vortices," *Progress in Aeronautical Sciences*, edited by D. Küchemann, Vol. 7, Pergamon Press, Oxford, 1966, p. 145.

¹⁵ Lowson, M. V., "Some Experiments with Vortex Breakdown,"

Journal of the Royal Aeronautical Society, Vol. 68, 1964, pp. 343-346.

¹⁶ Hall, M. G., "A New Approach to Vortex Breakdown," *Proceedings of the 1967 Heat Transfer and Fluid Mechanics Institute*, Stanford University Press, Palo Alto, Calif., 1967, pp. 319-340.

¹⁷ Bossel, H. H., "Vortex Computation by the Method of Weighted Residuals Using Exponentials," *AIAA Journal*, Vol. 9, No. 10, Oct. 1971, pp. 2027-2034.

¹⁸ Bossel, H. H., "Vortex Equations: Singularities, Numerical Solution, and Axisymmetric Vortex Breakdown," CR-2090, 1972, NASA.

Shear Stress and Turbulence Intensity Models for Coflowing Axisymmetric Streams

S. W. ZELAZNY,* J. H. MORGENTHALER,† AND D. L. HERENDEEN‡

Bell Aerospace, Division of Textron, Buffalo, N.Y.

Accurate predictions of the mean velocity field for data covering a wide range of conditions were made using an eddy viscosity model. Two key features of this model, developed by correlating turbulence intensity and shear in coaxial coflowing streams are: 1) a direct relationship between eddy viscosity and turbulence intensity is proposed and 2) the lateral distribution of eddy viscosity is specified. The model has accurately predicted the mean velocity and mass fraction distributions downstream of an injector element with initial conditions considerably outside the range from which the models were developed. Both low-speed and supersonic quiescent and coflowing jets have been successfully correlated; primary jet molecular weights range from 2.0 to 120.09. Data used was tested for consistency by comparing momentum and injected gas integral balances at each axial station. Comparisons between predicted and experimental mean velocities, mass fraction, shear stress and turbulence intensities are presented.

Nomenclature

a	= jet radius (Fig. 1)
a_1	= inner jet radius (Fig. 13)
a_2	= outer jet radius (Fig. 13)
D	= jet diameter (Fig. 1)
D_p	= density factor, Eq. (2d)
E	= mass defect, Eq. (2f)
L	= characteristic length, Eq. (2g)
R_{uv}	= shear correlation coefficient Eq. (6)
r	= radial coordinate (Fig. 1)
r_1	= value of r where $(U - U_e)/(U_j - U_e) = 0.999$
r_2	= value of r where $(U - U_e)/(U_j - U_e) = 0.001$
Sc_T	= turbulent Schmidt number
U	= mean velocity in z direction
u	= fluctuating velocity in z direction
u'	= $\langle u^2 \rangle^{1/2}$
u'/U_j	= axial turbulence intensity
v	= fluctuating velocity in r direction (or y direction for planar geometries)
v'	= $\langle v^2 \rangle^{1/2}$
W	= wake factor, Eq. (2e)
w	= fluctuating velocity in direction perpendicular to y and z
w'	= $\langle w^2 \rangle^{1/2}$
Y	= mean mass fraction of injected gas
z	= axial coordinate (Fig. 1)
z_c	= velocity core length (Fig. 1)

\bar{z}	= z/D
ϵ	= eddy viscosity, Eq. (1)
ζ	= r/r_u
ρ	= mean density
(ρv)	= fluctuating mass flux component in direction of v
τ_e	= Reynolds momentum flux (shear stress)
$\langle \rangle$	= time averaged quantity

Subscripts

c	= evaluated at $r = 0$
e	= evaluated at $r = \infty$
$e1$	= evaluated at $a_1 \leq r \leq a_2$ and $z = 0$ (Fig. 13)
$e2$	= evaluated at $r = \infty$ (Fig. 13)
j	= evaluated at $r = 0, z = 0$
u	= evaluated at velocity half radius, r_u
min	= minimum value at a given z
max	= maximum value at a given z

Introduction

THE ability to describe complex turbulent mixing phenomena is essential if the performance of systems such as rocket injectors, combustion lasers, scramjet combustors, and gaseous core nuclear rockets are to be modeled. In addition a mixing model which could predict details of the turbulence, i.e., turbulent shear and intensity could be used to predict aerodynamic jet noise. Of course prediction of the details of the turbulence is a more difficult problem than prediction of mean profiles. Once successful eddy viscosity models have been developed, a solution of the time-averaged continuity, momentum, species continuity and energy equations yield the complete flowfield, i.e., the mean velocity, injected gas concentration, and temperature distribution. From such solutions combustion efficiency and over-all performance may be computed. Consequently, parameters of concern to the design engineer, e.g., combustor length, may be estimated without resorting completely to the frequently

Presented as Paper 72-47 at the AIAA 10th Aerospace Sciences Meeting, San Diego, Calif., January 17-19, 1972; submitted March 29, 1972; revision received February 20, 1973. This work was supported in part by the Air Force Office of Scientific Research under Contract F44620-70-C-0116 with technical monitoring by B. T. Wolfson.

Index categories: Jets, Wakes, and Viscid-Inviscid Flow Interactions; Subsonic and Supersonic Airbreathing Propulsion.

* Research Scientist, Computational Continuum Mechanics. Member AIAA.

† Staff Scientist, High Energy Laser Technology. Member AIAA.

‡ Engineering Analyst; presently with Hughes Aircraft Company.

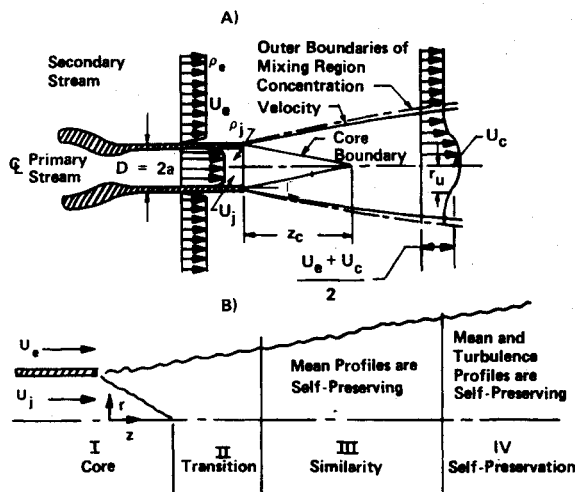


Fig. 1 Schematic of coaxial turbulent jet and definition of mixing regions.

employed trial-and-error approach. Guidance for the hardware designer is the ultimate goal of this work.

For the jet mixing problem considered herein (Fig. 1) in which there is a predominant flow direction, the equations of momentum, species continuity, and thermal energy may be simplified using boundary-layer approximations. In addition, the turbulent mass and heat fluxes in these equations generally have previously been related to the shear stress by assuming constant turbulent Schmidt and Prandtl numbers. Zelazny et al.¹ showed that this assumption is not generally valid in the transition region (Fig. 1).

Early mixing analyses obtained closed form solutions of these equations by employing the concept of jet similarity,^{2,3} and consequently, their results were only applicable far downstream, i.e., where the mean profiles were similar. More recently numerical techniques have been developed, e.g., see Ref. 4, with which solutions may be obtained throughout the flowfield if appropriate models for turbulent momentum, mass, and thermal energy fluxes are available. The major difficulty in obtaining solutions has been to accurately model these turbulent flux terms.

It is convenient to classify approaches taken in specifying the turbulent momentum flux (shear stress) into two categories. The more commonly used approach, designated category I, has been to specify an eddy viscosity model. Category II includes any method which introduces at least one additional equation to describe shear stress, e.g., the turbulent kinetic energy equation. Examples of the different forms these equations may take may be found in Refs. 6–12.

The objective of this investigation was to develop a reliable mixing model for regions downstream of the core, Fig. 1, which would accurately predict mean velocities for coflowing axisymmetric jets which covered a wide range of flow conditions, i.e., subsonic or supersonic speeds with density variations caused by gradients in one or more of the following: molecular weight, total temperature, or velocity. In addition the details of the turbulence would also be predicted. The axisymmetric geometry was chosen since it is most commonly encountered in systems of interest. Of the two approaches available, it was decided that developing an eddy viscosity model would be the more fruitful. The reasons for this choice are as follows.

1) A relatively large amount of data covering a wide range of flow conditions exists for this problem. Hence an empirical eddy

viscosity relationship can be developed which is not restrictive to a specific set of flow conditions.

2) The eddy viscosity approach does not require initial values of shear stress or turbulent kinetic energy as are required in most of the methods of category II. This information, unlike initial mean velocity, concentration, and temperature generally is not known.

Therefore when the eddy viscosity model developed herein is further generalized to apply to the core region calculations may be made from the point of injection without requiring shear stress profiles.

3) In case of the species diffusion and energy equations, a simple eddy diffusivity closure hypothesis, i.e., constant turbulent Schmidt and Prandtl number is generally inadequate.¹ Hence, the Reynolds transport terms should be modeled either semi-empirically, analogous to modeling the shear stress described herein, or by introducing additional equations analogous to the turbulence kinetic energy equation. Methods of category II seek to model the physics through closure of the turbulence equations at a higher level than the eddy viscosity approach. Therefore to be consistent, methods of category II, which for example might introduce an equation for the shear stress, should introduce equations for the turbulent mass and heat flux. Unfortunately, the experimental data required to specify the terms (second- and higher-order correlations involving mass temperature fluctuations) introduced in these equations is unavailable at this time. On the other hand, specifying semiempirical models for the eddy coefficients of mass and energy is completely consistent with the eddy viscosity concept.

4) The eddy viscosity approach is clearly simpler than methods of category II which have at least one additional equation; therefore, shorter computer running times will result.

5) Methods of category II may eventually produce a turbulence model applicable over a wide range of geometries and flow conditions[¶]; the ultimate would be a complete turbulence theory applicable to all types of flows. Nevertheless, the empirical model developed in this investigation at least will be useful when flow conditions of interest are within the range where the model has been shown to be applicable.

In the following sections the approach taken in developing the eddy viscosity model is presented. Its difference from earlier models is discussed, and a comparison of predicted mean velocities and turbulent intensities with published data presented. In addition, the model was used to analyze a practical problem of current interest, i.e., a coaxial gaseous H_2/O_2 rocket injector element applicable for the Space Shuttle Reaction Control System. The conditions used in this application are significantly different from those used to develop the model since mixing of three gases must be considered and a very heavy gas is exhausting into a much lighter gas. Areas where more experimental work is needed to enhance our understanding of axisymmetric coflowing turbulent streams are described.

Approach

Describing shear stress with an eddy viscosity model has had limited success in the past.¹ Consequently, a philosophy which differed from that previously used was followed in this investigation. These differences were: 1) accurate data covering a relatively wide range of flow conditions were used to develop this eddy viscosity model, 2) emphasis was placed in accurately correlating with the shear stress rather than only mean values, and 3) the empirical constants in the model were determined by optimizing the correlation of all experimental data considered rather than a single case.

Probably one of the most important requirements of a model is proper prediction of the maximum shear stress, $(\tau_e)_{\max}$ at each downstream station. This maximum value is important because

§ The approach itself is not new as it was suggested by Prandtl.⁵ A slightly different approach was taken by Nee and Kovasznay⁶ in which a rate equation for the eddy viscosity, rather than the shear stress, was developed based on physical arguments.

¶ See Refs. 8 and 9 for examples of how methods of category II have accurately predicted downstream flowfields when initial shear stresses were available.

Table 1 Relationship between u' and v'

Investigator	Conditions	v'/u' at	
		$r = 0$	$r = r_u$
1. Sami ¹⁹	Incompressible quiescent jet. Data at $\bar{z} = 1, 3, 6$, and 10.	0.84	0.707
2. Wagnanski and Fiedler ²⁰	Incompressible quiescent jet. Data at $\bar{z} > 20$.	0.88	0.72
3. Gibson ²²	Incompressible quiescent jet. Data at $\bar{z} = 50$.	0.98	0.75
4. Townsend ²³	Incompressible wake of circular cylinder. Data in region of self-preservation.	1.16	0.88
5. Zawacki and Weinstein ¹⁸	Incompressible coflowing jets. Wakelike since jet velocity usually much less than freestream velocity. Data at $0 \leq \bar{z} \leq 21.0$.	0.73 ^a	0.57 ^a

^a Average values of 4 cases reported.

τ_e is zero on the centerline and freestream where $(\partial U/\partial r) = 0$. The primary objective of Ref. 1 was to develop an expression for $(\tau_e)_{\max}$ (assumed to be at the velocity half width) which correlated shear stress data over a wide range of flow conditions. This model (reviewed in the next section) was an important first step in the development of the more general model developed in this study which gives the detailed variation of τ_e across the jet, i.e., includes radial as well as axial variation. Since this investigation is a continuation of the work reported in Ref. 1, the pertinent results of that study are summarized below.

1) The most commonly used eddy viscosity models were tested and shown to be completely inadequate for predicting shear stress in many of the flows.

2) Many of the shortcomings of past models were avoided in the development of this model, i.e., rather than using mean values of velocity, turbulent shear stresses were correlated. The data used¹³⁻²⁰ were tested by checking the consistency of the integral balances of total mass, injected mass, and momentum (only 18 of 33 cases treated were considered sufficiently accurate, Table I of Ref. 1). Finally the range of flow conditions considered covered a broader spectrum than previous studies.

3) A model for shear stress and turbulence intensity at the velocity half width was developed by correlating the 18 accurate sets of data.

Derivation of the General Model

The general behavior of τ_e and u' for all values of r and z was determined by starting with the definition of the Reynolds stress and introducing the shear correlation coefficient and eddy viscosity in the conventional manner^{2,12}

$$\tau_e = -\langle(\rho v)u\rangle = \rho R_{uv} u'v' = \epsilon \partial U/\partial r \quad (1)$$

It should be noted that the effects of fluctuations in density are assumed negligible in Eq. (1). This assumption has been shown to be valid for compressible flows (up to Mach numbers as high as three) in which the molecular weight is constant.²¹ To date, no information regarding the effect of neglecting density fluctuations in flows of variable molecular weight is available. However, the good agreement between predicted and experimental mean profiles obtained using the eddy viscosity model developed below suggests that for the conditions studied the effect is not very important.

The models for the shear stress and turbulence intensity** developed in Ref. 1 were generalized in the present investigation. The maximum value of the shear stress, assumed in Ref. 1 to occur at the velocity half width, was given by

$$(\tau_e)_u = 0.018[(1+2f)D_p WE/L](\partial U/\partial r)_u \quad (2a)$$

** It was necessary to develop a model for turbulence intensity in order to obtain a $(\tau_e)_u$ model.

where the shear correlation coefficient at $r = r_u$ which was used in arriving at Eq. (2a) was given by

$$(R_{uv})_u = -0.15(1+2f)/f^{1/2} \quad (2b)$$

The ratio of $v'^2/u'^2 = f$ is given by

$$f = (0.5+0.005\bar{z}) \quad \bar{z} < 100; \quad f = 1.0 \quad \bar{z} \geq 100 \quad (2c)$$

The factor D_p and W accounting for large-density differences between the primary and secondary streams and flows which are wakelike ($U_e > U_j$) were given, respectively, by

$$D_p = (\rho_u/\rho_{\min})^{1.5} \quad (2d)$$

and

$$W = 1.0 + \exp(-4.61U_j/U_e) \quad (2e)$$

The mass defect E and characteristic length L were given by

$$E = \int_{r_1}^{r_2} |\rho U - \rho_e U_e| r dr \quad (2f)$$

and

$$L = r_u + (2a - r_u) \exp(-0.115\bar{z}) \quad (2g)$$

Using these equations, the turbulence intensity can be written as

$$(u'/U)_u = 0.346[(D_p WE/\rho_u LU_u^2)(\partial U/\partial r)_u]^{1/2} \quad (3)$$

Details on how the radial variations of τ_e , u' , v' , and R_{uv} were empirically modeled is presented below.

Relationship between u' and v'

Results of anemometry measurements of low-speed, single gas quiescent jets,^{19,20,22} wakes,²³ and coflowing jets¹⁸ are shown in Table 1. As expected, the relationship between u' and v' depends on the flow conditions and region of interest. For purposes of developing an empirical eddy viscosity model for both incompressible and compressible flows, it is reasonable to assume as a first approximation that the variation in v'/u' is negligible across the mixing region and can be approximated by its value at the velocity half width in the transition and similarity regions. The added refinement of including a radial variation is not warranted in light of the spread in data for u' and ϵ (see Figs. 3 and 4). Consequently, Eq. (2c) may be applied for all values of r and z .

The effect of density variations due to either the mixing of gases of different molecular weights or compressibility have not been reflected in this relationship [Eq. (2c)], since hot-wire data for these conditions are not available. This fact suggests that additional-empirical relationships, e.g., D_p [Eq. (2d)], must be introduced when attempting to correlate data where density variations are significant. Note that these empirical relationships reduce to a value of unity for conditions corresponding to those from which Eqs. (2b) and (2c) were developed.

Relationship for R_{uv}

Harsha and Lee²⁴ have found that a large number of free shear layer flows satisfy

$$\langle uv \rangle = 0.15(u'^2 + v'^2 + w'^2) \quad \text{at } r \approx r_u \quad (4)$$

where $v' \approx w'$ for axisymmetric flows. Harsha⁸ in applying the turbulence kinetic energy approach to predict free mixing flows found it necessary to assume††

$$\langle uv \rangle = 0.15(u'^2 + v'^2 + w'^2) \frac{\partial U}{\partial r} \left/ \left(\frac{\partial U}{\partial r} \right)_u \right. \quad (5)$$

which correctly predicts the shear at the centerline, half width and freestream. As will be shown, a consequence of Eq. (5) is the eddy viscosity, ϵ is proportional to $\rho u'^2$. Combining Eqs. (1, 4, and 5) and using the assumption that u'/v' does not vary with r yields

†† Harsha⁸ applied Eq. (5) for the region $0 \leq r \leq r_u$ and Eq. (4) for $r > r_u$. In this study, an eddy viscosity approach was used and consequently the velocity gradient introduced in Eq. (5) was retained for all r , which is consistent with the argument⁸ that Eq. (4) is no longer valid in regions where the shear vanishes but the turbulence kinetic energy is finite.

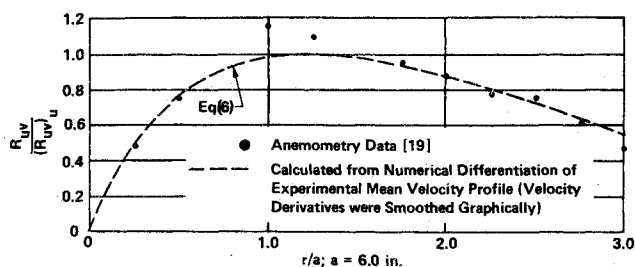


Fig. 2 Variation of the shear correlation coefficient across the mixing region (Ref. 19, $z/D = 10.0$).

$$R_{uv} = (R_{uv})_u \frac{\partial U}{\partial r} \bigg/ \left(\frac{\partial U}{\partial r} \right)_u \quad (6)$$

A test of this relationship may be made by comparing the experimental shear correlation coefficient with its value predicted from differentiation of the mean velocity profile. The data of Sami¹⁴ is one of the few references which report data in sufficient detail to make such a comparison possible. Figure 2 shows that Eq. (6) gives fair agreement with the data (maximum difference of 14%) in describing the variation of R_{uv} about $(R_{uv})_u$. Comparisons were also made at $\bar{z} = 1, 3$, and 6 and showed that in the core region ($\bar{z} = 1$ and 3) and immediately downstream of the core ($\bar{z} = 6$) this relationship does not apply. Efforts to model the core region will be documented in a future paper.

As in the development for a relationship between u' and v' , it must be noted that the data used to develop Eqs. (2b) and (6) does not reflect the effect of density variations. Such effects can be incorporated by introducing empirical relations developed by correlating shear stress of variable density flows.

Relationship for $\rho u'^2$

Equations (2c, 3, and 6) may be combined to yield

$$\tau_e = \rho (R_{uv}) f^{1/2} u'^2 \frac{\partial U}{\partial r} \bigg/ \left(\frac{\partial U}{\partial r} \right)_u \quad (7)$$

and using Eq. (2a) and (3)

$$\frac{\tau_e}{(\tau_e)_u} = \frac{\rho u'^2}{(\rho u'^2)_u} \left(\frac{\partial U}{\partial r} \right) \bigg/ \left(\frac{\partial U}{\partial r} \right)_u \quad (8)$$

or defining the function $G(r, z)$

$$G(r, z) = \rho u'^2 / (\rho u'^2)_u = \varepsilon / \varepsilon_u \quad (9)$$

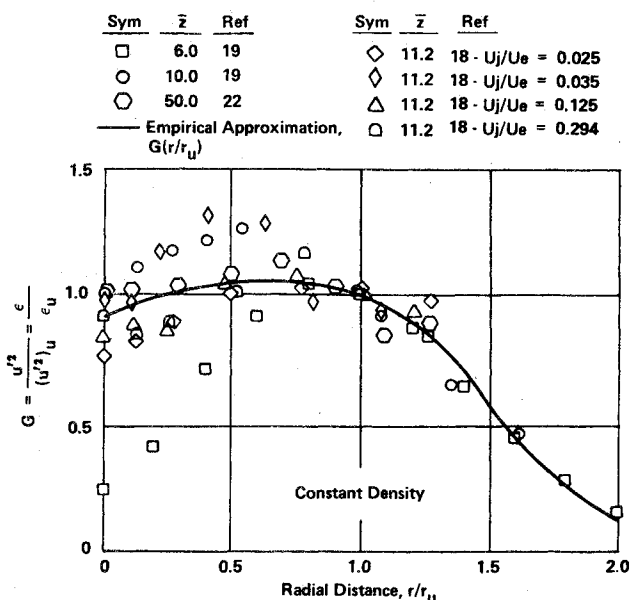


Fig. 3 Radial distribution of axial component of turbulent kinetic energy and eddy viscosity; constant density flows.

Sym	\bar{z}	r_u (in.)	ε_u (lbm/ ft-sec)	Ref
○	6	7.350	0.0296	19
□	12.6	0.780	0.120	15
◇	10.3	0.303	0.272	13 - $U_j/U_e = 6.30$
◆	12.5	0.400	0.0385	13 - $U_j/U_e = 4.40$
+	5.6	0.354	0.00135	18 - $U_j/U_e = 0.294$
△	5.6	0.389	0.000611	18 - $U_j/U_e = 0.185$
▲	8.4	0.456	0.000608	18 - $U_j/U_e = 0.132$

— Empirical Approximation, $G(r/r_u)$

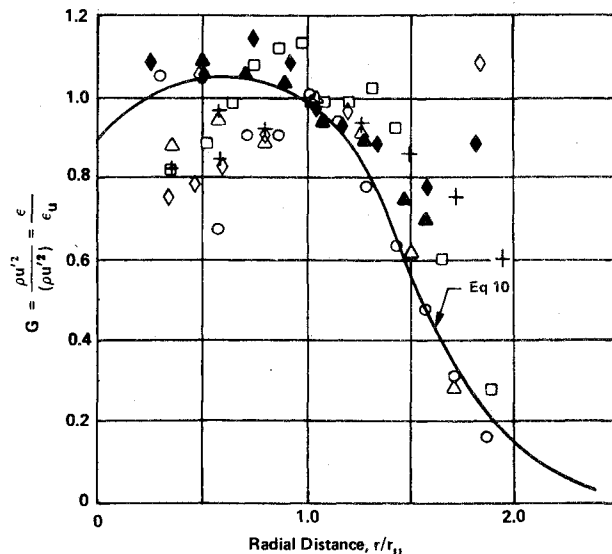


Fig. 4 Radial distribution of axial component of turbulent kinetic energy and eddy viscosity; variable density flows.

Data for both u'^2 for incompressible flows and ε for both constant and variable density flows were used to develop the empirical expression $G(r, z)$. Figure 3 shows the data of Refs. 18, 19, and 22 for $u'^2/(u'^2)_u$ where $\rho = \text{const.}$ †† From these data it is clear that G must monotonically decrease for $\zeta > 1$. The specific behavior of G in the region $0 \leq \zeta \leq 1$ is not as well-defined due to the lack of self-preservation (see Fig. 1) of the turbulence quantities, i.e., if the flows were self-preserving all data would rest on a single curve.

The effects of density variations across the mixing region on G are reflected in the ratio $\varepsilon/\varepsilon_u$. Figure 4 shows this ratio for a representative number of the cases considered. A careful examination of these results showed that no single consistent trend could be found which was correlated with the density variation across the mixing region. Although the specific behavior of G in the region $0 \leq \zeta \leq 1$ is not well-defined these data, like those of Fig. 3, do indicate that G does not vary significantly from unity and peaks somewhere at $\zeta < 1.0$. This result implies that in both constant and variable density flows the eddy viscosity reaches a maximum at some distance from the centerline and exhibits an intermittent behavior at the outer edge of the mixing region. As a simple first approximation for G , the function given by Eq. (10) was developed and is plotted as a solid curve in Figs. 3 and 4. This function was chosen because it gave a reasonable representation of the mean value of the data. Use of techniques such as least squares fit seemed unwarranted because of the excessive scatter.

†† Data for the turbulence quantities in Ref. 18 have been shown to be lower than the real values^{1,2,9} therefore the usefulness of the data is questionable. On the other hand only the general shape of u'^2 across the mixing region is of interest and the data may be used for this purpose if it is assumed that the measurements are uniformly low. This seems reasonable since the data¹⁸ exhibits a behavior not too different from the data of Refs. 19 and 22.

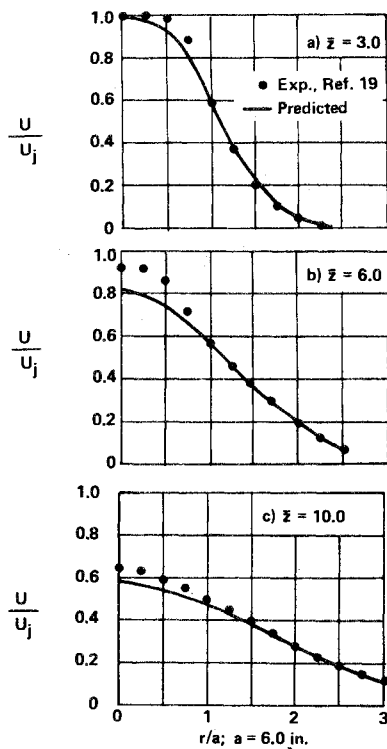


Fig. 5 Experimental and predicted velocity profiles.

$$G(\zeta) = \frac{1.05 - 0.15 e^{-4.6\zeta}}{1 + 0.05\zeta^7} \quad (10)$$

General Models for τ_e and u'

Substituting for each of the terms of Eq. (1) yields the following new mixing model for shear stress in the transition region of coflowing jets:

$$\tau_e = 0.018[(1+2f)D_p WEG/L] \partial U / \partial r \quad (11)$$

The turbulent intensity relative to the initial jet mean velocity is given by

$$u'/U_j = 0.346[(D_p WEG/\rho LU_j^2)(\partial U / \partial r)]^{1/2} \quad (12)$$

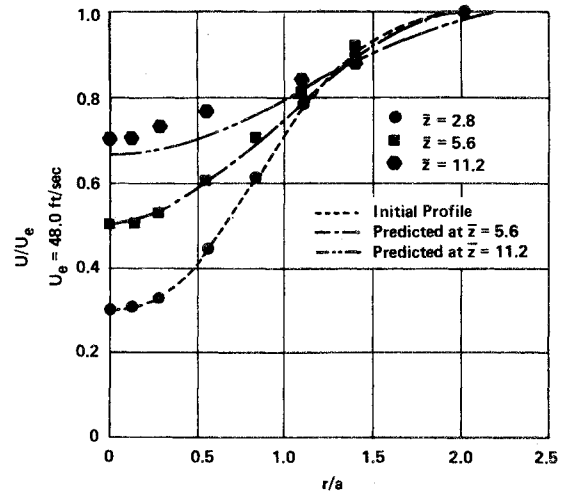
where the functions f , $D_p W$, E , L , and G have been defined by Eqs. (2c-g) and (10).

Equations (11) and (12) have been used to predict shear stress, turbulence intensity and mean velocity fields. Typical predictions of these are shown in the following sections.

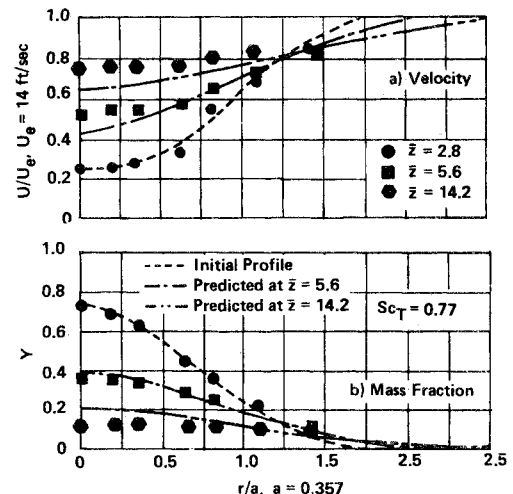
Predictions Using the Model

Predictions were made for the mean values (velocity, mass fraction and temperature), shear stress and axial turbulent intensity for the cases which had consistent integral balances, i.e., 18 of the 33 (see Table I of Ref. 1). The governing equations were solved numerically in von Mises coordinates^{§§} using an explicit finite-difference method.²⁵ Comparisons of predicted and experimental data were made for all eighteen cases and reported in Ref. 26. The complexity of the region immediately downstream of injection (core region) requires special consideration in any jet mixing analysis. Therefore, in this study the data used to develop the model is primarily for axial stations downstream of the core region.

§§ Since the equations are solved in von Mises coordinates a singularity is introduced when the velocity becomes zero, e.g., a submerged jet. This singularity was avoided by making the freestream velocity small but finite (1% of the initial jet velocity). The effect of the finite velocity on the predictions was found to be negligible for the distances downstream considered.

Fig. 6 Experimental and predicted velocity profiles. Symbols denote data of Ref. 18, $U_j/U_e = 0.294$.

It was found that in 17 of the 18 cases the difference between experimental and predicted mean velocity was within 20%. For the data of Alpinieri¹⁷ the model predicted mixing to be significantly lower than indicated by experiment.^{¶¶} Comparisons with experimental shear stress for all 18 cases was possible since this parameter was obtained either directly from anemometry data or indirectly from an inverse solution to the momentum equation in which experimental data were differentiated once and the transport coefficient determined. Details of this inverse solution method may be found in Refs. 27 and 28. In this study it was found that the difference between experimental and predicted maximum shear stress was within 30% in 7 cases and within 80% in 14 of the 18 cases. This degree of accuracy appears sufficient since the mean velocity was accurately predicted and many of the more common eddy viscosity models have been shown to often incorrectly predict the shear stress by as much as 400%.¹ Figures 5-12 show some of the comparisons of predicted and experimental mean velocity, mass fraction, as well as shear stress and turbulent intensity for cases that are representative of the results and conditions being considered.

Fig. 7 Experimental and predicted velocity and freon mass fraction profiles. Symbols denote data of Ref. 18, $U_j/U_e = 0.132$.

¶¶ This singular case suggests that the experimentally observed high rate of mixing might be attributed to unusually high freestream turbulence levels which are assumed negligible by the model.

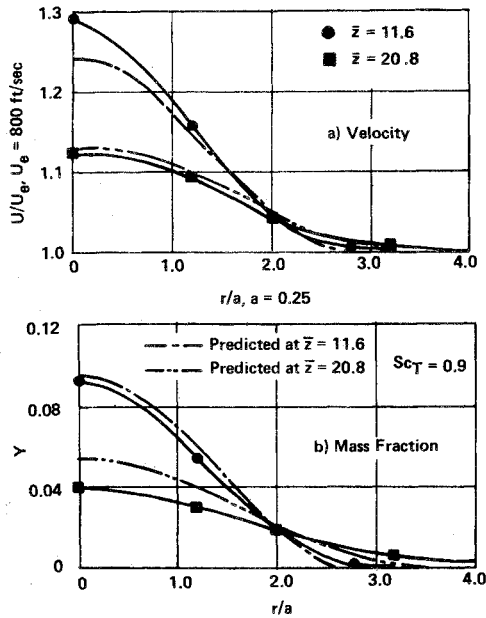


Fig. 8 Experimental and predicted velocity and hydrogen mass fraction profiles. Solid line through symbols designates smooth data (symbols are not data points). Data of Ref. 13, $U_j/U_e = 3.0$.

Mean Profiles

Prediction of the mean velocity for the classical incompressible submerged jet was made and compared with the data Sami¹⁸ where detailed results are reported in the core region ($\bar{z} = 1$ and 3) and in the transition region ($\bar{z} = 6$ and 10). Efforts to start calculations in the core region were not successful for most of the cases considered indicating that in general a modification to the empirical expressions is required in this region. One exception to this result was the data of Ref. 19. For this case it was found that when calculations were started in the transition region, $\bar{z} = 6$, the predicted mean velocity, $\bar{z} = 10$, was in good agreement with the data (within 2% error), whereas reasonable agreement was also obtained when calculations were started in

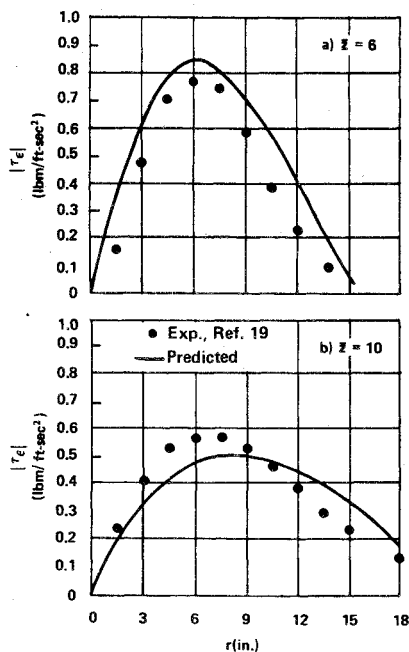


Fig. 9 Experimental and predicted shear stress profiles.

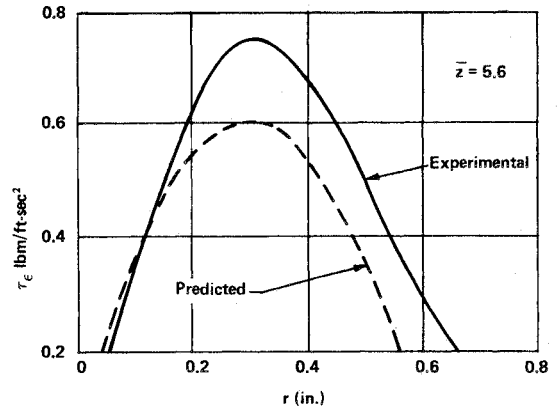


Fig. 10 Experimental and predicted shear stress profiles. Data of Ref. 18, $U_j/U_e = 0.294$.

the core region, $\bar{z} = 1$. The results for calculations made starting in the core region are shown in Fig. 5.

Predictions for the wakelike, constant density jet of Ref. 18 gave very good agreement (within 7% error) with data, Fig. 6, whereas predictions for the wakelike variable density jet,¹⁸ Fig. 7, were in somewhat poorer agreement (17% maximum error for mean velocity and 80% maximum error for mean mass fraction of freon). The turbulent Schmidt number used to obtain the mass fraction predictions (Figs. 7 and 8) was obtained from the inverse solution of the species continuity equation, i.e., the same method used to calculate the shear stress. The value chosen was a composite average of the calculated Sc_T (which varied both radially and axially). A constant value was chosen as a first approximation, but Fig. 7 suggests that better agreement with experimental mean values of Y could be obtained by allowing Sc_T to decrease with increasing \bar{z} ; the turbulent diffusion of mass would increase thereby lowering the predicted Y which would result in better agreement with data at $\bar{z} = 14.2$.

Predictions of the mean velocity and hydrogen mass fraction are shown in Fig. 8 and are compared with the data of Ref. 13. As in the preceding case reasonable agreement was obtained for the mean velocity (3% maximum error); whereas, the mean hydrogen mass fraction prediction was in poorer agreement with the data (33% maximum error). This result again demonstrates the need for an independent mass transfer coefficient model (rather than assuming a constant Schmidt number). Development of an empirical model for Reynolds mass transfer currently in progress will remove the need for specifying a constant Sc_T .

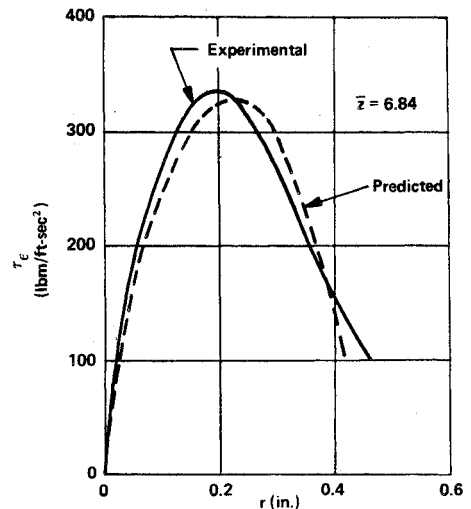
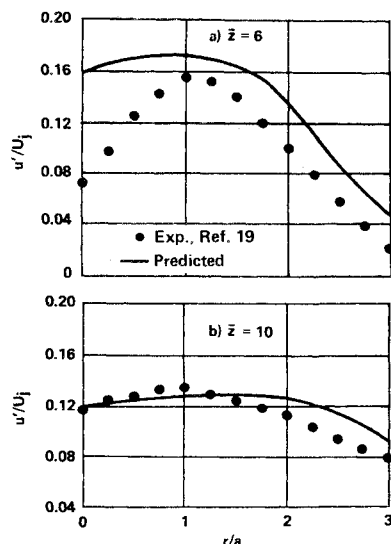


Fig. 11 Experimental and predicted shear stress profiles. Data of Ref. 13, $U_j/U_e = 3.0$.

Fig. 12 Experimental and predicted axial turbulence intensity profiles.



Turbulence Quantities

A comparison between predicted shear stress and experimental values measured directly, i.e., using a hot wire, is shown in Fig. 9 for the data of Sami.¹⁹ Good agreement was obtained near the point of maximum shear (20% maximum error) but poorer agreement was obtained near the regions of low shear, i.e., the centerline and freestream. However, these results did not significantly affect the accuracy of the predicted mean velocity (Fig. 5). Comparisons between the predicted and experimental shear stress¹⁸ are shown in Fig. 10. The predicted shear stress had a maximum error of 20% near the peak experimental value. As was found in the previous case, the size of the discrepancy between predicted and experimental shear stress did not significantly affect the predicted mean velocity. The predicted and experimental shear stress for the high-speed hydrogen jet of Ref. 13 is shown in Fig. 11. Good agreement was obtained although the point of maximum shear is somewhat shifted towards the outer edge of the mixing region.

Predictions of the turbulent intensity are presented in Fig. 12 and compared with the data of Sami¹⁹ (the only set of detailed turbulent intensity data* which was found in the literature for the axisymmetric turbulent jet for the region of interest). Good agreement was obtained at $\bar{z} = 10$ (20% maximum error), whereas²⁵ poor agreement was obtained near the centerline for $\bar{z} = 6$. An examination of the turbulence intensity and mean velocities for this case show that the mean velocity core has disappeared at $\bar{z} = 6$ but the turbulent intensity core [herein defined as that z station where $u'_c < 0.9(u')_u$] is still present. The

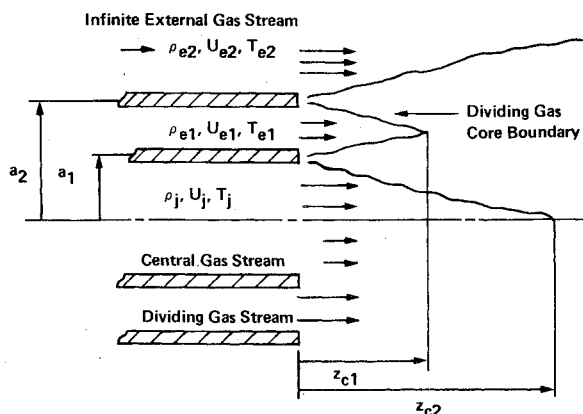


Fig. 13 Three stream coaxial axisymmetric jet.

* The data of Ref. 18 was excluded for aforementioned reasons.

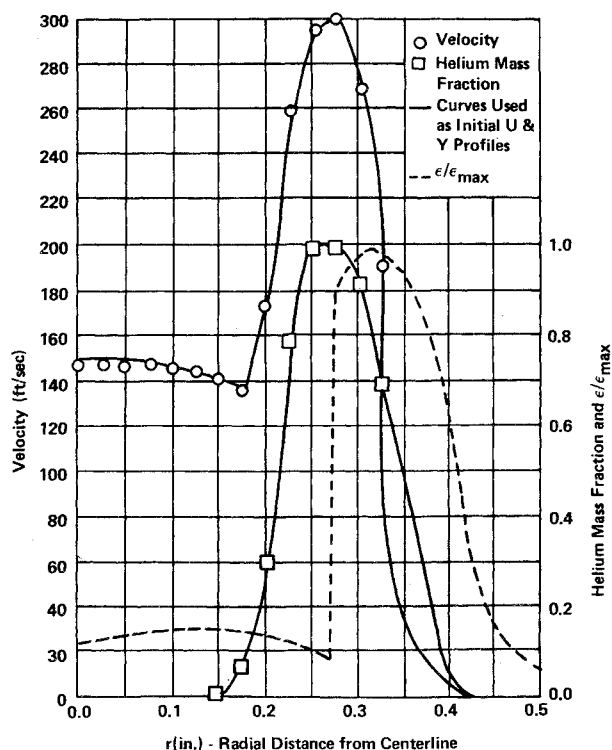


Fig. 14 Initial velocity, helium mass fraction and eddy viscosity profiles at $z = 0.394$ (1.0 cm). Symbols denote data of Ref. 30. Smooth curves used as initial profiles.

fact that the turbulence intensity core persists further downstream than the mean velocity core must be considered when modeling the core region, but was beyond the scope of this paper. However, efforts are in progress to model the core region and preliminary results suggest incorporating an axial dependence in the function $G(\zeta)$, (other than already included through r_u) will significantly improve the predicted values at $\bar{z} = 6$ without significantly changing the already accurate predictions at $\bar{z} = 10$.

Three Stream Coaxial Jet

Clearly the usefulness of any empirical relationship is demonstrated only when it is successful in correlating data other than that used in its development. An even more severe test is to determine its ability in correlating data with conditions far outside the range from which it was developed. Figure 13 illustrates such a problem, i.e., a nitrogen gas jet exhausting into a thin annular ring of helium which is mixing with the surrounding air. This configuration simulates a coaxial gaseous H_2/O_2 rocket injector element of interest for Space Shuttle Reaction Control Systems.

The three important differences between these conditions and those used to develop the model are: 1) mixing of three gases must be considered, hence the second stream may not be assumed infinite in extent, 2) the density ratio between the primary gas, N_2 and secondary gas He are outside the range of the data used to develop the model, and 3) the region of interest is less than five external diameters downstream, i.e., the furthest station downstream is 3.34 in. and the external diameter is 0.68 in.

The model was tested by starting numerical integration from the initial station ($z = 0.394$ in.) using experimental profiles³⁰ shown in Fig. 14 and predicting downstream profiles. Since the model was developed for two stream jets, it was necessary to apply it in two regions for this configuration. The dividing point between the two regions was chosen where the velocity reached its maximum value. No adjustment was made to any of the empirical constants. Predicted eddy viscosity profiles are shown in Figs. 14 and 15.

Predicted velocity and helium mass fraction profiles were compared with the experimental values, Fig. 15. Results show that these predictions are in good agreement with the data and demonstrate that the model can be a useful tool by giving a reasonably accurate prediction of flowfield development.

Conclusions

An eddy viscosity model was developed and shown to be a useful tool for predicting mean velocity and concentration profiles for coaxial turbulent jets covering a wide range of flow conditions. Predictions were made for both subsonic and supersonic flow in which density variations were caused by variation in molecular weight, total temperature, or velocity. The model was successful a) in accurately predicting the mean velocity field for the 18 coaxial jet cases considered and b) in successfully modeling a three stream coaxial H_2/O_2 gaseous rocket injector element. The successful modeling of this injector element is encouraging since the flow conditions and geometry were outside the range from which the model was developed; however, this initial success is not a general demonstration of the universality of the model. Nevertheless, it suggests that the model can be extended somewhat beyond the condition for which it was developed.

Reasonably successful empirical models for the shear stress and turbulent intensity were developed along with the eddy viscosity model. The relations for τ_e and u' , although sufficiently accurate for describing the mean values, did not yield equally accurate predictions of the turbulence quantities. No doubt improved correlation of the shear stress and turbulent intensity can be obtained by introducing additional correlating functions. The

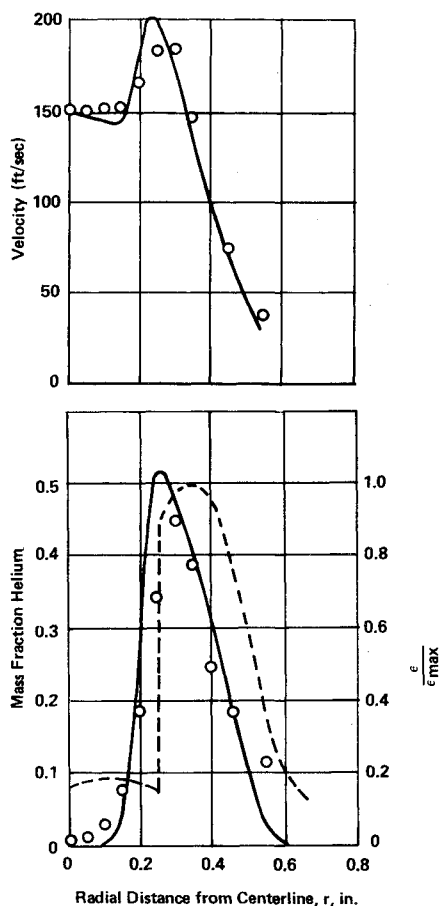


Fig. 15a Experimental (○) and predicted (—) velocity and helium mass fraction profiles and eddy viscosity (---) profile at $z = 1.389$ in., data of Ref. 30.

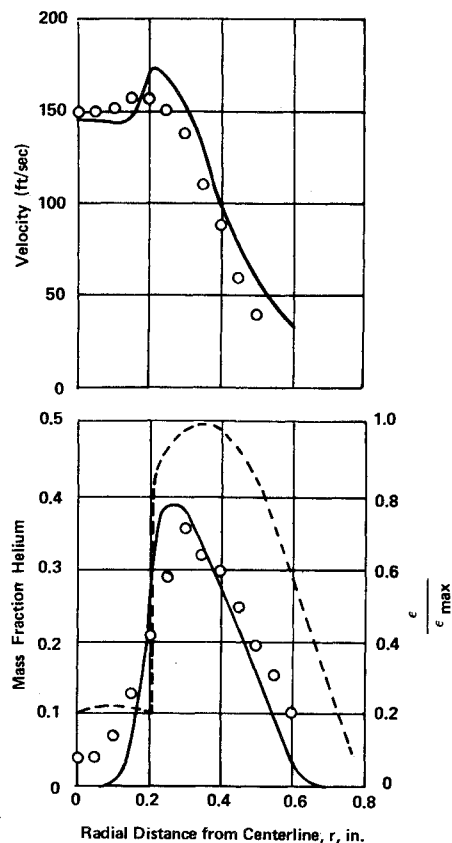


Fig. 15b Experimental and predicted velocity, helium mass fraction profiles and eddy viscosity (---) profile at $z = 1.97$ in., (○) experimental data of Ref. 30, (—) predicted.

general approach used herein to develop an empirical model for the Reynolds shear stress and eddy viscosity should be used to develop independent models for turbulent mass and energy transport, so that each of the transport processes can be modeled independently; i.e., turbulent Schmidt, Prandtl and hence Lewis numbers do not have to be specified.

Future turbulent jet experimental studies should investigate the effect of the following variables on the flowfield development: a) pressure gradients and pressure levels other than near atmospheric; b) initial conditions; c) heavy gas jets exhausting into light gases, e.g., oxygen into hydrogen; d) jet to freestream velocity ratios near unity.

References

- 1 Zelazny, S. W., Morgenthaler, J. H., and Herendeen, D. L., "Reynolds Momentum and Mass Transport in Axisymmetric Coflowing Streams," *Proceedings of the Heat Transfer and Fluid Mechanics Institute*, 1970, pp. 135-153.
- 2 Pai, S. I., *Fluid Dynamics of Jets*, Van Nostrand, New York, 1954.
- 3 Abramovich, G. N., *The Theory of Turbulent Jets*, MIT Press, Cambridge, Mass., 1963.
- 4 Patankar, S. V. and Spalding, D. B., *Heat and Mass Transfer in Boundary Layers*, Morgan-Gampiar, London, 1967.
- 5 Prandtl, L., "On a New Representation of Fully Developed Turbulence," publ. 13, 1952, Translated by D. Coles, Jet Propulsion Lab., Pasadena, Calif.
- 6 Nee, V. W. and Kovaszny, L. S. G., "Simple Phenomenological Theory of Turbulent Shear Flows," *The Physics of Fluids*, Vol. 12, Pt. 3, 1969, pp. 473-484.
- 7 Patankar, S. V. and Spalding, D. B., "A Finite Difference Procedure for Solving the Equations of the Two Dimensional Boundary Layer," *International Journal of Heat and Mass Transfer*, Vol. 10, 1967, pp. 1389-1412.
- 8 Harsha, P. T., "Free Turbulent Mixing: A Critical Evaluation of

Theory and Experiment," Ph.D. dissertation, Dec. 1970, Univ. of Tennessee, Knoxville, Tenn.; also AEDC TR 71-36, Feb. 1971, Arnold Engineering Development Center, Tenn.

⁹ Bradshaw, P., Ferriss, D. H., and Atwell, N. P., "Calculation of Boundary Layer Development Using the Turbulent Kinetic Energy Equation," *Journal of Fluid Mechanics*, Vol. 28, Pt. 3, 1967, pp. 593-616.

¹⁰ Harlow, F. H. and Nakayama, P. L., "Turbulence Transport Equations," *The Physics of Fluids*, Vol. 10, Pt. 1, 1967, pp. 2323-2332.

¹¹ Donaldson, C. du P., "A Computer Study of an Analytical Model of Boundary-Layer Transition," *AIAA Journal*, Vol. 7, No. 2, Feb. 1969, pp. 271-278.

¹² Hinze, J. O., *Turbulence*, McGraw-Hill, New York, 1959.

¹³ Chriss, D. E., "Experimental Study of Turbulent Mixing of Subsonic Axisymmetric Gas Streams," AEDC-TR-68-133, Aug. 1968, Arnold Engineering Development Center, Tenn.

¹⁴ Zakkay, V., Krause, F., and Woo, S. D. L., "Turbulent Transport Properties for Axisymmetric Heterogeneous Mixing," PIBAL, Rept. 813, March 1964, Polytechnic Inst. of Brooklyn, N.Y.

¹⁵ Eggers, J. M., "Velocity Profiles and Eddy Viscosity Distributions Downstream of a Mach 2.2 Nozzle Exhausting to Quiescent Air," TN 3601, Sept. 1966, NASA.

¹⁶ Eggers, J. M. and Torrence, M. G., "An Experimental Investigation of the Mixing of Compressible Air Jets in a Coaxial Configuration," TN D5315, July 1969, NASA.

¹⁷ Alpinieri, L. J., "Turbulent Mixing of Coaxial Jets," *AIAA Journal*, Vol. 2, No. 9, Sept. 1964, pp. 1560-1568.

¹⁸ Zawacki, T. S. and Weinstein, H., "Experimental Investigation of Turbulence in the Mixing Region Between Coaxial Streams," CR-959, Feb. 1968, NASA.

¹⁹ Sami, S., "Velocity and Pressure Fields of a Diffusing Jet," PhD dissertation University Microfilms 67-2672, 1966, Univ. of Iowa, Ames, Iowa; also *Journal of Fluid Mechanics*, Vol. 27, 1967, pp. 231-252 and Vol. 29, 1967, pp. 81-92.

²⁰ Wagnanski, I. and H. Fiedler, "Some Measurements in the Self

Preserving Jet," D1-82-0712, April 1968, Boeing Scientific Research Labs.; also *Journal of Fluid Mechanics*, Vol. 38, 1969, pp. 577-612.

²¹ Bradshaw, P. and Ferriss, D. H., "Calculation of Boundary Layer Development Using the Turbulent Energy Equation. II Compressible Flow on Adiabatic Walls," NPL AERO Rept. 1217, Nov. 1966, England.

²² Gibson, M. M., "Spectra of Turbulence in a Round Jet," *Journal of Fluid Mechanics*, Vol. 15, 1963, pp. 161-173.

²³ Townsend, A. A., "The Fully Developed Turbulent Wake of a Circular Cylinder," *Australian Journal of Scientific Research*, Vol. 2, pp. 451-468.

²⁴ Harsha, P. T. and Lee, S. C., "Correlation Between Turbulent Shear Stress and Turbulent Kinetic Energy," *AIAA Journal*, Vol. 8, No. 8, 1970, pp. 1508-1510.

²⁵ Zelazny, S. W., Morgenthaler, J. H., and Slack, M. S., "Spatial Dependence of Turbulent Transport Coefficients in Dissimilar Coaxial Flows," Rept. 9500-920123, March 1969, Bell Aerospace Co., Buffalo, N.Y.

²⁶ Zelazny, S. W., Morgenthaler, J. H., and Herendeen, D. L., "Shear Stress and Turbulent Intensity Models for Coflowing Axisymmetric Streams," Rept. 9500-920211, in preparation, Bell Aerospace Co., Buffalo, N.Y.

²⁷ Morgenthaler, J. H., "Supersonic Mixing of Hydrogen and Air," CR-747, April 1967, NASA; also summarized in *International Journal of Heat and Mass Transfer*, Vol. 9, 1966, pp. 1401-1418.

²⁸ Morgenthaler, J. H., "Mixing in High Speed Flow," Rept. 9500-920114, Aug. 1968, Bell Aerospace Co., Buffalo, N.Y.

²⁹ Lee, S. C. and Harsha, P. T., "Use of Turbulent Kinetic Energy in Free Mixing Studies," *AIAA Journal*, Vol. 8, No. 6, June 1970, pp. 1026-1032.

³⁰ Fricke, H. D., private communication, 1971, Bell Aerospace Co., Buffalo, N.Y.; data summary Fricke, H. D. and Schorr, C. J., "Measurement of Gaseous Mixing Downstream of Coaxial and Adjacent Orifices," *Journal of Spacecraft and Rockets*, Vol. 9, No. 8, Aug. 1972, pp. 563-564.